EVALUATING 3-D SIGHT DISTANCE AT URBAN INTERSECTIONS USING A LIDAR-BASED MODEL AND CONSIDERING MULTIPLE USERS

Gonzalez-Gomez Keila[1], Iglesias-Martínez Luis[2], Rodríguez-Solano Roberto[3], Castro María[4]
[1,4] Depto. de Ingeniería Civil: Transporte y Territorio, E.T.S.I. de Caminos, Canales y Puertos, Universidad Politécnica de Madrid, Madrid, Spain
[2] Depto. de Ingeniería Geológica y Minera, E.T.S.I. de Minas y Energía, Universidad Politécnica de Madrid, Madrid, Spain
[3] Depto. de Ingeniería y Gestión Forestal y Ambiental, E.T.S.I. Montes, Forestal y Medio Natural, Universidad Politécnica de Madrid, Spain

Abstract: The provision of sufficient available sight distance along the road reduces the potential for conflicts among its users. Consequently, sight distance estimations are significant components of road safety analyses. Evaluating sight distances on existing roads, when not performed in situ, requires up-to-date representations of the roads' geometric properties and roadside elements. For some time now, LiDAR instruments have been used to gather geospatial data needed to generate updated models of the roadways and roadside elements. Digital terrain models (DTM) have been widely utilized to perform sigh distance estimations, despite the fact that these models only account for the road surface and bare terrain. On the other hand, Digital Surface Models (DSM) which provide further information of features, namely vegetation, traffic signs, buildings and other manmade elements, yield inaccurate results when some elements protrude or project over roadway areas like cantilevered signs, tree branches and in the presence of complex above ground features. The authors have previously proposed a methodology to overcome this inaccurate representation of road assets and surrounding elements utilizing Geographic Information System (GIS) tools and 3-D geometries on top of the DTM so as to represent possible visual obstructions. In this analysis, the available sight distance of an urban intersection located in Madrid (Spain), is evaluated considering its prevalent motorized vehicles. Virtual trajectories of pedestrians and cyclists were modelled in order to assess the impact of road surrounding objects in their available sight distance. Furthermore, the separate consideration of 3-D objects allows the possibility of assisting decision making processes concerning the location of urban furniture while assuring proper visibility.

Keywords: LiDAR-derived models, Intersection sight distance, GIS, road safety.

1. Introduction

As it has been stressed in road geometric design guidelines, in order to make road transportation safe and efficient, drivers ought to have the ability to visually discern lengths of road ahead so as to perform specific maneuvers effectively (AASHTO, 2011; Fomento, 2016). Crossing, stopping and passing are just some of the driving tasks that require adequate distances to be accomplished safely and for which road transportation agencies have defined minimum values. These values are meant to be compared against the available sight distance (ASD) and based on their comparison, when requirements are not met, measures are taken, or actions performed. Amongst the different kinds of road elements and settings, at-grade urban intersections are considered to be one of the most complex sections, given that they usually include high traffic volumes and multiple road users in a variety of movements including conflictive ones (AASHTO, 2011). In this sense, by providing sufficient intersection sight distances (ISD) designers intend to allow drivers to identify potentially conflicting vehicles, physical elements and non-motorized users. Along with the ISD, sufficient stopping sight distance (SSD) is a key feature of safe intersection functioning.
Sight distances provided during the design stage are to be verified on in-service roads given that possible changes on speed limits could occur and considering the dynamic nature of road surroundings. These measurements can be carried out in situ, statically (with operators on the road measuring maximum unobstructed sight lines) or dynamically (car following another while checking sight distance values). Off-site estimations have mainly been executed utilizing photo or video-logging and Mobile Mapping Systems (MMS). Some of these procedures consider horizontal and vertical alignment separately which several researchers have found to possibly misestimate the existent ASD (Hassan et al., 1996; Ismail and Sayed, 2007).
With respect to roadside features, urban roads environs experience changes from existing or new vegetation, manmade structures and also from the recent increase, in dimensions and amount, of street furniture as a result of higher connectivity and smartness in several cities.
When measuring the ASD on existing roads off-site and making use of 3-D geospatial data, accurate representations of the road geometric definition and roadside elements are needed and might be obtained from many sources. In recent times, LiDAR systems have been intensively used to acquire information of the roads given that they allow the rapid acquisition of up-to-date and precise data. This scanning technology has shown to be very useful and able to provide georeferenced data with enough resolution and coverage area to perform many transportation analyses. For these and other reasons many authors have utilized LiDAR derived products to carry out ASD estimations. Some of these authors have utilized the resulting point cloud to perform the calculations on them (Campoy Ungria, 2015; González-Jorge et al., 2016) and others generate 3-D models (Castro et al., 2011; de Santos-Berbel et al., 2014; Gargoum, 2017). Researchers making use of digital models can be differentiated by the type of model employed; some utilize Digital

[1] Corresponding author: keila.gonzalez.gomez@upm.es

Terrain Models (DTM's), which only represent the road geometry and bare ground, and others make use of Digital Surface Models (DSM's) which include roadside features along with the terrain. In view of the fact that some data structures used to store DSM's only show one elevation per planimetric position, Iglesias-Martinez et al., (2016) proposed the use of 3-D objects on top of the DTM's in order to establish a more realistic representation of the road and roadside features. Not only this proposed procedure allows the simulation of feature location or removal, useful to evaluate their possible effects on overall sight distance, but also makes possible the consideration of different trajectories. This permits the inclusion of non-motorized road users such as pedestrians and cyclists in the analysis.

The use of Airborne Laser Scanning (ALS), Terrestrial Laser Scanning (TLS) and Mobile Laser Scanning (MLS) systems has been widespread in the transportation field for some time now. Within the literature on sight distance estimations utilizing LiDAR scanners one can notice that each of these systems have been employed: ALS (Khattak et al., 2003; Khattak and Shamayleh, 2005; Castro et al., 2015), MMS (González-Jorge et al., 2016; Olsen et al., 2016) and TLS (Jung et al., 2018). Each system benefits from their different capture mode, area covered, point cloud distribution among other characteristics. In this regard, this study makes use of a TLS's given that urban intersections tend to suffer from elements obstructing the laser beam's way to the pedestrian area and segregated cycling infrastructure due to parked vehicles, passing pedestrians, vegetation, bus stop shelters and other street furniture elements, when covered with MMS.

Considering these facts, the main goal of this paper is to evaluate the available sight distance of an urban intersection, taking into account its prevalent users. This is accomplished exploiting the geoprocessing model based on GIS tools presented by Iglesias-Martinez et al. in 2016 and making use of TLS acquired LiDAR data. In order to account for its main users, as well as their potential obstructions, distinct trajectories and scenarios have been set up. Roadside features are modelled as 3-D objects obtained from a LiDAR-derived model and also as adaptations of tridimensional objects acquired from online libraries.

This paper is organized as follows: the next section provides a description of the procedure utilized, case study, scenarios and users. Results are shown in the third section, and lastly the conclusions.

2. Materials and Methods

As previously mentioned, intersections are complicated road areas requiring reciprocal visibility between users. In order to ensure that accurately, a 3-D procedure that gauges the impact that roadside elements could have on their visibility is carried out. Just as intersection design requires, this evaluation covers the functional roadway and adjacent sidewalks. Resulting ASD values are to be compared with the required stopping and intersection distances in order to assess how safely these maneuvers could be performed in the study area.

2.1. Procedure

The overall methodology comprises the projection of lines-of-sight from the indicated observer to distinct targets, its own path and conflict points. As described by Iglesias-Martinez (2016), this procedure makes use of geospatial analysis functionalities from the ArcGIS software, mainly the Line Of Sight and Construct Sight Line tools. Based on these and other functionalities, a geoprocessing model was built utilizing the ModelBuilder application, also from ArcGIS. This model obtains the observer and target points' precise coordinates from the given trajectory, defined by equally spaced points, and calculates if the terrain surface, road configuration or any aboveground feature interrupts the line of sight from observer to target. The process is carried out launching sight rays repeatedly from the observer's path and onward.

The data required to implement the procedure encompasses the observer's trajectory, the digital model, and optionally 3-D objects standing as potential obstructions. The observer's trajectory was depicted by the theoretical paths of a car, cyclists and pedestrians, defined for each possible movement at the case study intersection. These paths were digitalized from existing cartography of the road and in conjunction with the well-defined cross slope of the road, whose camber indicated its centerline, acquired from the point cloud-derived DTM. The terrain model utilized was generated from the LiDAR point clouds, scanned utilizing the TLS system Leica C10. The equipment was placed in planned locations around the intersection so as to cover the area of interest. These planned location's coordinates were obtained from a prior GNSS survey. Horizontal and vertical point spacing was set to be 0.05 m. The resulting cloud contained 39.1 million points. After the data pre-processing stage, carried out utilizing the software Leica Cyclone 9.0, the resulting registered and georeferenced point cloud was processed utilizing the software MDTopX (Digi21, 2018). Points classified as ground were utilized to generate the DTM. In addition to the DTM, a 3-D multipatch file was obtained from the point cloud encompassing aboveground features such as foliage, surrounding vegetation, street assets and traffic signals (fig. 1). The multipatch geometry, developed by Esri in 1997, is a geospatial data format utilized to portray the outer surface of three-dimensional features (Esri, 2018). The traffic signal and bus stop, considered to be potential obstructions, were obtained from 3-D objects libraries, adjusted to their real measurements (from field measurements), and inserted in their exact position as multipatch files. These modifications were performed utilizing SketchUp (Trimble, 2018) and the positioning in ArcScene.

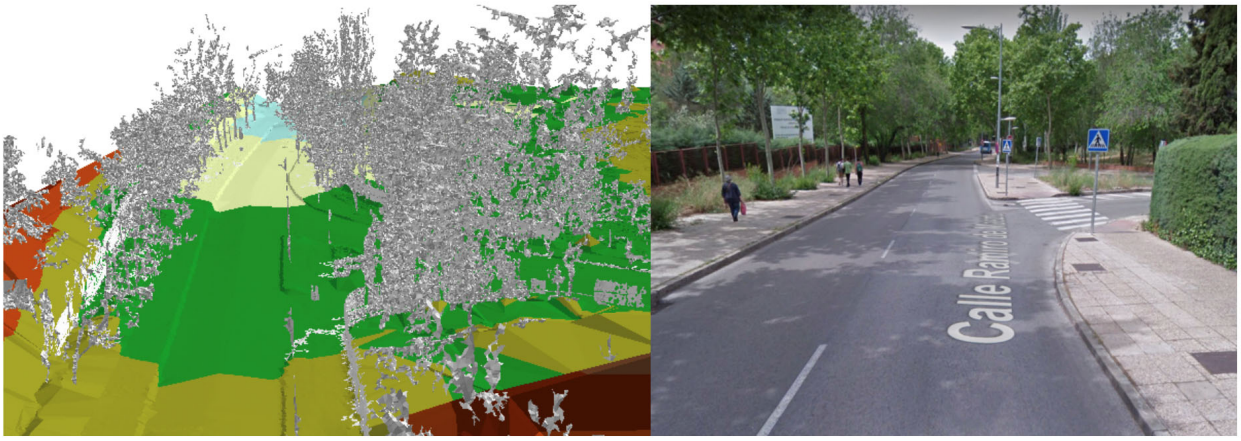

Fig. 1.
Multipatch on top of DTM (grey features)

2.2. Case Study

The 3-way, skewed intersection under study is located in the university district of Madrid (Spain). Intersecting roads are the one-way Ramiro de Maeztu (main road) and the two-way Moreras av. Both roads encompass a mean width of ~6.55 m and posted speed limit of 40 km/h. This raised channelized junction is controlled with stop signals on the minor road. Given the geometry of the intersection and the presence of a one-way road, only right turns and merging movements are possible, hence only diverging and merging conflict points were analyzed. Along the intersection's functional area, the horizontal alignment of both roads is composed by straight segments forming a ~62º skew angle junction. Regarding the vertical alignment, both roads feature grades of 5.3% and 4.2% respectively. This downgrade along Ramiro de Maeztu contributes to operating speed increases, which could reduce the user's time to anticipate and avoid potential conflicts. Figure 2 presents, on the left, an orthogonal and rotated view of the intersection and on the right its conflict points and possible movements. Stop, pedestrian crossing and diverging road signs are located around pedestrian-to-vehicle conflict points, before the minor-to-major road right turn, and in the channelization. The intersection's functional area contains two bus stops along both streets. One is a bus stop shelter and the other is a timetable displayer pole.

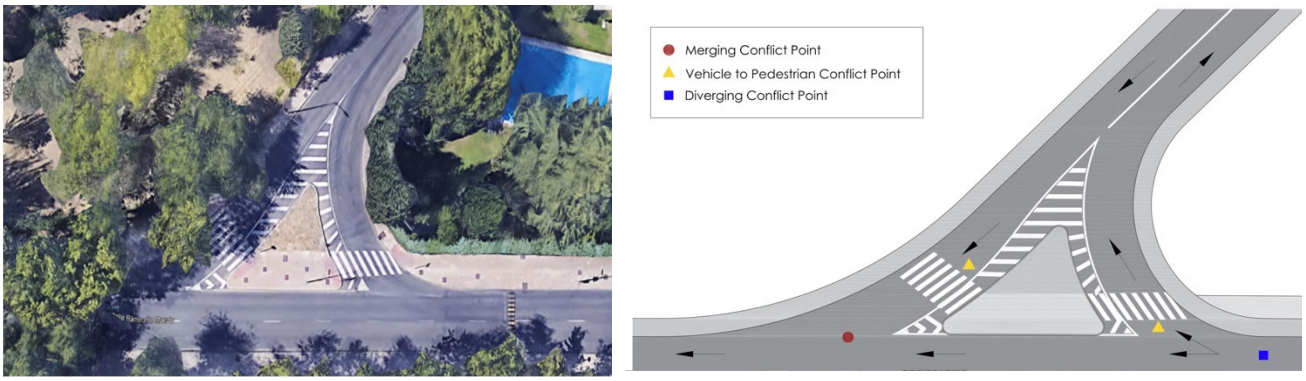

Fig. 2.
Junction under study

As abovementioned, all possible turns at the intersection were evaluated for its customary users and their potential obstructions. Its main users were considered to be pedestrians, cyclists, and passenger cars. Buses were not evaluated due to the advantages in visibility their driving height provides. As typical of an intersection located in a university district, customary pedestrians, transit users, and cyclists are mainly students.
Pedestrians trajectories were defined in the center of the sidewalk. The eye's height of a mobility impaired pedestrian was set to be at 1.5 m high plus another height of 1.7 m.
When sharing the road, cyclists are advised to transit in the center of the lane, but one must consider their meandering movement, required to maintain balance, which will be smaller with greater speeds. For regular speeds, between 15 km/h and 30 km/h, it is considered that the width needed by a cyclist in motion is 1.00 m. Taking these facts into account, two trajectories 1.00 m apart from the center of the lane were contemplated as the virtual trajectories of cyclists, at a height of 1.4 m as specified in the Guide for the Development of Bicycle Facilities (AASHTO, 2012). Drivers trajectories were placed 1.5 m away from the left inner side of the lane.

The first set of cases analyzed correspond to a straight downhill trajectory through Ramiro de Maeztu's street (blue arrow fig.3a). Here, the visibility of observers going downward is assessed in other to determine if the bus stop or traffic signs prevent them from noticing an approaching vehicle downward the Moreras street (red arrow fig. 3a). The second set of cases assessed observers turning right from Ramiro de Maeztu. Here the proper spotting of the pedestrian's crossings was assessed (fig. 3b). The third set of cases evaluated the visibility of observers going into Ramiro de Maeztu's street from Moreras (blue arrow fig. 3c). It was evaluated whether reciprocal visibility among them was provided and if the bus stop-shelter or street signals had any or important effects on it. Forth set of cases assessed pedestrians' visibilities with trajectories defined along the sidewalk; this case evaluated from which distance oncoming vehicles were spotted by distinct types of pedestrians. All sets contemplated 3 scenarios; the first one without bus stop-shelter, so as to evaluate its impact on the junction's functioning, the second one with the bus stop-shelter located at its exact coordinates and a third case where the bus stop is located where it provides the best overall visibility. The bus stop-shelter evaluated is located 35 m from the intersection in the direction sketched in fig 3a.

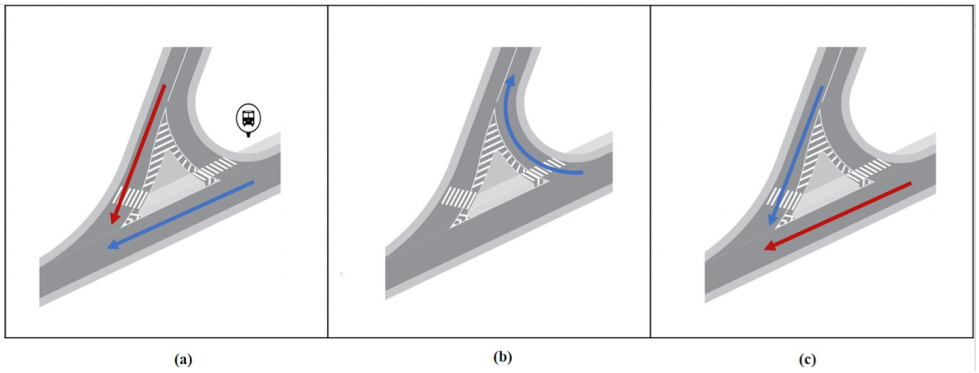

Fig. 3.
Turns under study

Both stopping sight distance (SSD) and intersection sight distance (ISD) where evaluated for drivers and cyclists, comparing calculated values to available ones. Stopping sight distances were carried out considering the observer's height above the roadway at 1.08 m, and that of the target at 0.6 m (AASHTO, 2011). When contemplating a cyclist, the target's height was considered to be 0.15 m (AASHTO, 2012). The SSD was determined in consistency with the expression provided by the AASHTO, equation 1.

$$SSD = 0.278V_t + \frac{V^2}{254\left[\left(\frac{a}{9.81}\right) \pm G\right]} \quad (1)$$

Where: V is the design speed; t is the brake reaction time of 2.5 s; a is the deceleration rate of 3.4 m/s and G the downgrade slope.
As stipulated in the guidelines, clear sight triangles providing a free view of the entire intersection are fundamental for its correct functioning. This triangle was assessed for the right turning from the minor road. The departure point of the triangle on the minor road (Moreras) is recommended to be from 4.4 to 5.4 m from the edge of the major road, according to field observations (AASHTO, 2011). The length of the triangle is defined as the total distance from the main road plus half its lane width (for vehicles approaching from the left); the base of the triangle is defined by the ISD, which can be determined according to the expression provided by the AASHTO (equation 2).

$$ISD = 0.278\, V_{major} t_g \quad (2)$$

Where V_{major} is the design speed of the major road and t_g is the time wrap for minor road vehicle to enter the major road, which is stipulated to be 6.5 s for passenger cars.

3. Results

This section presents the main findings of the evaluation. A total of 36 cases with different combinations of users, turns and potential obstructions were calculated and are introduced as follows: first SSD results, subsequently the ISD's and lastly pedestrians'. SSD assessments were aimed at locating any obstacle, from the road geometry or roadside elements, that could hamper the observer's perception of a specified target on their path. ISD focused on assessing the observer's

capacity of visualizing conflict points which could be on their traversed road or not. Evaluation of pedestrians assessed the possibility of noticing approaching vehicles from a reasonable distance.

3.1. SSD

Stopping sight distance values were obtained for each road utilizing their posted speed limit and downward/upward slope, these values are displayed in table 1. Passenger car drivers' SSD was obtained at 40 km/h and that of the cyclists 30 km/h.

Table 1
Required SSD along the intersection

Observer	Calculated SSD downward main road (m)	Calculated SSD (m) upward minor road	Calculated SSD (m) downward minor road
Drivers	49.03	44.01	48.48
Cyclists	44.06	40.21	43.63

Sight-distance graphs are shown and discussed below for the least favorable cases; each chart shows stations on the horizontal axis and the ASD on the vertical. Figure 4 shows on the left considered stations and the right displays results. The ASD obtained is shown for two scenarios, the blue line denotes those obtained considering the bus stop-shelter and the red one shows the distances obtained without it. The green line exhibits the calculated-required SSD. As seen the turn is provisioned with enough SSD and the impact of the shelter is not substantial, hence scenario 2, with the bus stop relocated, was not presented. Cyclists evaluations carried out for this movement showed similar results, provisioning of the SSD and not exceptional differences caused by the bus stop.

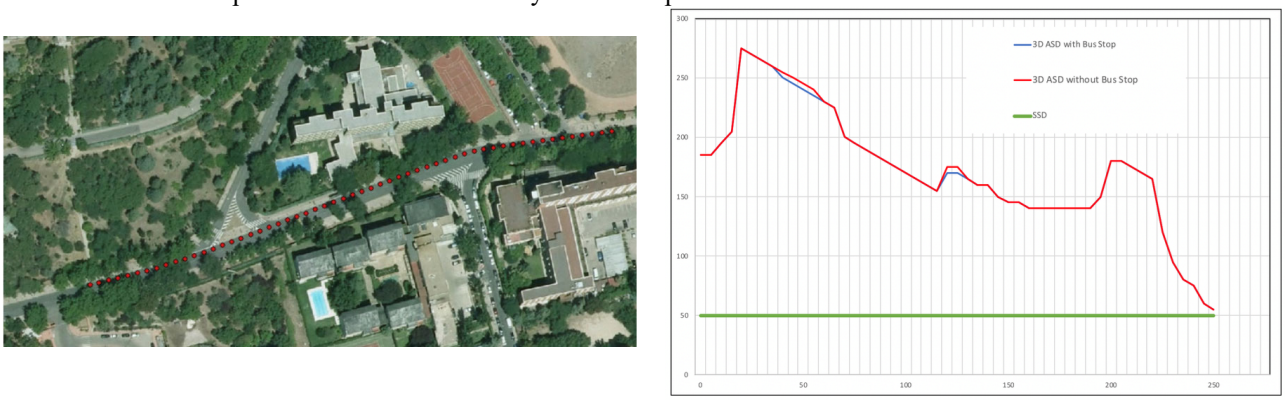

Fig. 4.
Results of the SSD estimations for observers downhill main road

The defined trajectory for the second set of cases, which considered drivers and cyclists turning left from the main road, is displayed in fig. 5 (left). On the right, the outcomes of drivers through the right turning. As before, the blue line shows the values of the ASD estimated considering the bus stop-shelter and the red without its inclusion. The graph shows a logical decrease in the ASD values due to the horizontal curve and roadside vegetation. Cyclists showed similar outcomes for their two considered trajectories, decreasing ASD as approaching the turning and sudden increasing after it.

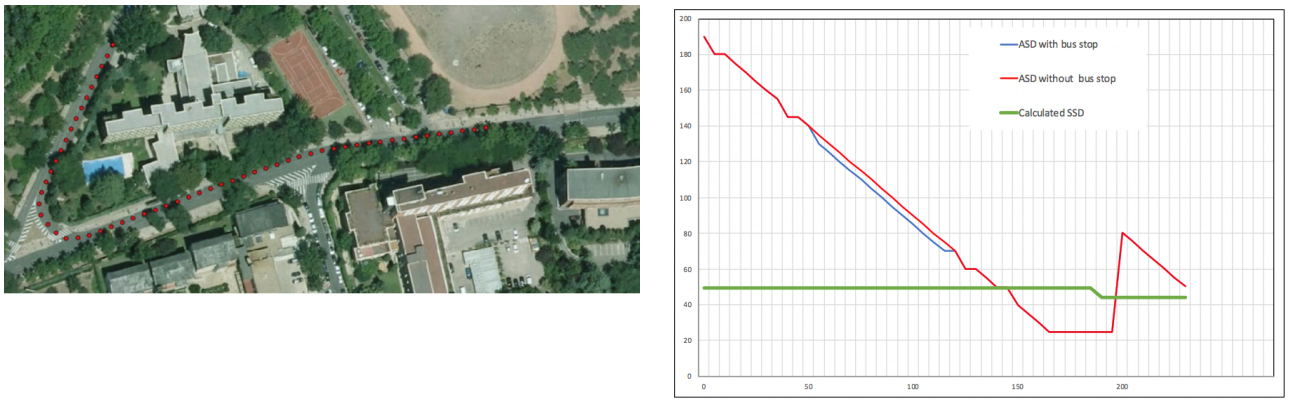

Fig. 5.
Trajectory and SSD results of observers turning right the main road

The third set of cases, which evaluated drivers and cyclists turning right from the minor road is illustrated in figure 6. These graphs show the results of the two trajectories considered for cyclists, both 1 m apart from the center of the lane. It shows reductions in the ASD due to lack of clearance this horizontal curve has. Generally speaking they show the same tendency but differences of 5 and even 10m of visibility arise at some stations.

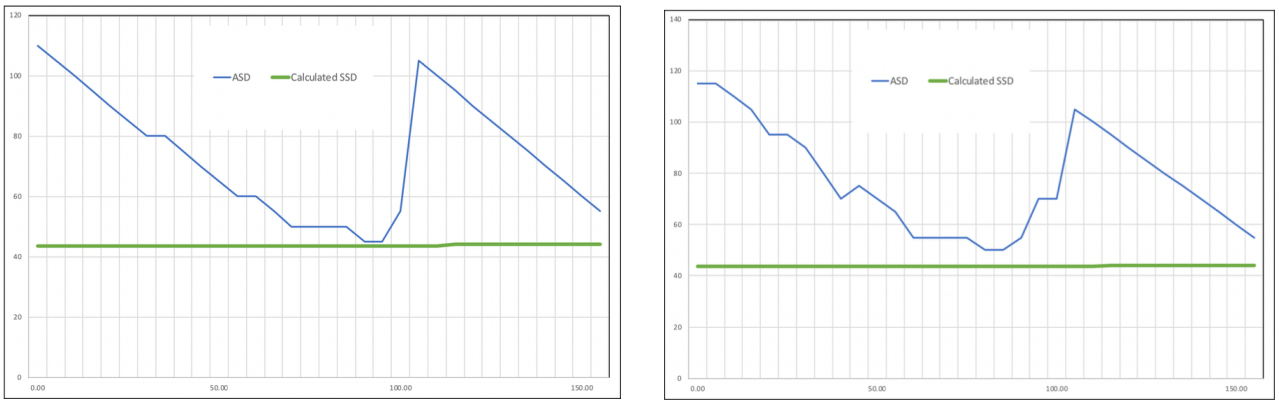

Fig. 6.
SSD estimations considering cyclists turning right from the minor road

3.2. ISD

Departure sight triangles were calculated for the minor road left turn. Also, the estimation of the visibility of conflict points along the different set of cases. These estimations were calculated utilizing object heights of 1.08m, 1.5m and 1.7m (eye's height of drivers and pedestrians, being the objects to be seen).
For the first set of cases, the existence unobstructed lines-of-sight was determined from the driver's and cyclists' paths to the merging conflict point. In addition, a sightline evaluation was performed towards the stop area on the minor road. Results were calculated setting the observers at a distance of 50-70m away from the conflict point. Outcomes showed that all observers were able to spot oncoming vehicles in the stop area, but the bus stop-shelter prevents cyclists riding near the curb to perceive approaching drivers which are located 10-20m before the stop sign.
The second set of cases assessed whether drivers could spot pedestrians crossing at an adequate distance. Results verified that uphill or downhill pedestrians are spotted right in the crossing and before it; both 1.70m and 1.50m are clearly spotted. These results are important because downhill pedestrians could forget to look back for oncoming vehicles before starting to cross. For cyclists, given that their trajectory is prone to more variation within the lane, the proper spotting of pedestrians 50m away from the crossing depends on the location of the pedestrian on the crossing and the position of the cyclist on the lane, due to the bus stop-shelter and crossing sign. A third scenario where the bus station was moved 5 m uphill from the intersection revealed improved visibility values.
The third case estimated the provisioning of a clear sight triangle for approaching traffic down the stop-controlled minor road. The decision point, spot where the driver should start the stopping maneuver, was placed 4.4m from the major road; the base of the triangle was located in the center of the lane, given that vehicles are approaching from the left and the third point was located using the resulting ISD, 72.28m. Figure 7 illustrates the sight triangle. The ISD is pointed at, and inside the triangle are the lines-of-sight projected from the driver's location to stations located on the trajectory of oncoming traffic. All shown lines are unobstructed, hence the sight triangle is provisioned. Additionally, considering the fact that the pedestrian crossing is right before the right turn, drivers will most likely reduce their speed before approaching the turn. ISD for cyclists was found to be 63.24 m and showed similar outcomes.

3.3 Pedestrians' Visibility

Unlike drivers and cyclists, pedestrians do not count with well stablished formulae aimed at the estimation of the sight distances required for their maneuvers (Eassa, 2016).

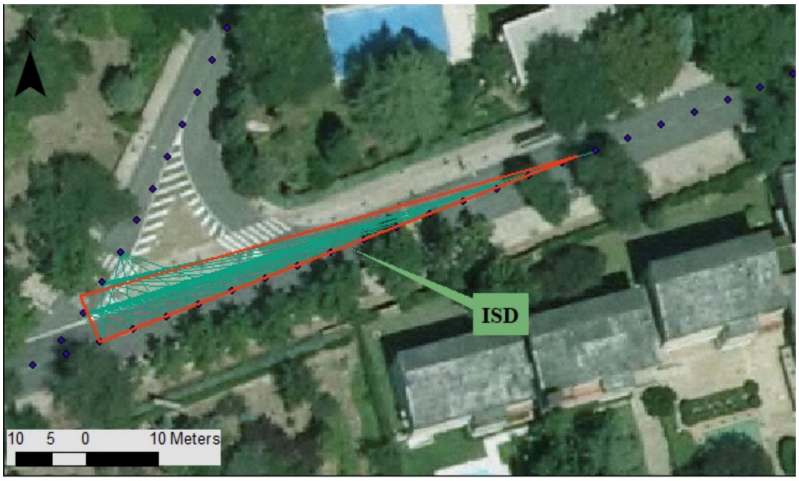

Fig. 7.
Departure sight triangle for the minor road

Sightlines were projected on the pedestrians' path aiming at approaching vehicles. Stations were separated 1m apart contemplating the average stride length and the variability of wheelchairs. Observers evaluated were able to spot oncoming traffic at a distance of 50m from the intersection along both roads. The first pedestrian crossing encounters drivers downwards from Moreras St. and are provisioned with more than 50m of visibility uphill. This was estimated for both ends of the crossing. The second pedestrian crossing provides sufficient visibility for users going upwards, being the bus stop-shelter the hindering element at about 60m. Pedestrians going downwards the main road must look back for oncoming vehicles, which is usually done fast and not carefully.

4. Conclusions

The provisioning of an adequate ASD is indispensable for creating safe driving conditions. Given that urban road intersections include distinct road users and maneuvers, road engineers should provide design elements aiming at reducing potential erratic operations. In this sense, giving the number of elements surrounding urban streets, utilizing a 3-D approach helps to determine the real effect in the visibility that they could infer, and not to mention the possible misestimations that 2-D evaluations might have. In this sense, so as to represent the road environment in the more realistic approach, this procedure permits to utilize DTMs in combination with files containing aboveground features captured by the LiDAR. These represented objects could be manmade elements, vegetation, street furniture and more. This procedure offers important functionalities regarding these potential obstructions. When it comes to urban street furniture and signalization, since these elements' dimensions are straightforwardly known, and effortlessly obtainable as 3-D objects files, the evaluation of the best positioning in terms of safety is achievable.
Urban streets are designed to accommodate distinct users and modes of transport, with this in mind the presented procedure included pedestrians and cyclists. The number of cyclists sharing the roads is increasing, and cities are fostering these attitudes in different ways but not always considering that many urban roads were designed to fulfil requirements of motor vehicles and should be evaluated to accommodate others. Furthermore, sight distances of mobility impaired pedestrians are often obviated. In this sense, results from the estimation of cyclists ASD evidenced how even a slight change in the positioning along the lane produces changes in the visibility and also the possibility of vehicles to spot other users. Pedestrian's maneuvers are often neglected and just as drivers do, pedestrians take many decisions on their crossing behavior based on what they are able to see and infer from the road. These decisions affect directly on drivers maneuvers hence the importance on reciprocal visibility.

Acknowledgements

The authors gratefully acknowledge the financial support of the Spanish Ministerio de Economía y Competitividad and European Regional Development Fund (FEDER). Research Project TRA2015-63579-R (MINECO/FEDER).

References

AASHTO. 2011. *A Policy on Geometric Design of Highways and Streets*. AASHTO. USA, 934 p.
AASHTO. 2012.*Guide for the Development of Bicycle Facilities*. AASHTO. USA.
Campoy-Ungria, J. M. 2015 *Nueva Metodología Para La Obtención De Distancias De Visibilidad Disponibles En Carreteras Existentes Basada En Datos Lidar Terrestre*. Doctoral dissertation Universitat Politècnica de València. Spain. 325p.
Castro, M.; Iglesias, L.; Sánchez, J. A.; Ambrosio, L. 2011.Sight distance analysis of highways using GIS tools, *Transportation Research Part C: Emerging Technologies*, 19(6): 997–1005.

Castro, M.; Garcia-Espona, A.;Iglesias, L. 2015 .Terrain Model Resolution Effect on Sight Distance on Roads, *Periodica Polytechnica Civil Engineering*, 59(2): 165–172.
De Santos-Berbel; C., Castro; M., Lopez-Cuervo; S., Paréns-González, M. 2014. Sight distance studies on roads: influence of digital elevation models and roadside elements. *Procedia - Social and Behavioral Sciences* 160: 449–458.
Digi21. 2018. Modelos Digitales Topográficos MDTopX. Available from internet: <https://www.digi21.net/MDTop>.
Easa, S. M. 2016. Pedestrian Crossing Sight Distance, *Transportation Research Record: Journal of the Transportation Research Board* 2588: 32–42.
Esri. 2018. Multipatches. Available from internet: <http://desktop.arcgis.com/en/arcmap/latest/extensions/3d-analyst/multipatches.htm>.
Gargoum, S. A. 2017.Automated Assessment of Sight Distance on Highways Using Mobile LiDAR Data. In *Proceedings of the Conference of the Transportation Associatio*n. Canada. 1–16.
González-Jorge, H.; Díaz-Vilariño, L.; Lorenzo, H.; Arias, P. 2016. Evaluation of Driver Visibility from Mobile Lidar Data and Weather Conditions, *International Archives of the Photogrammetry, Remote Sensing and Spatial Information Science*s, 577–582.
Hassan, Y.; Easa, S. M.; El Halim, A. O. A. 1996. Analytical model for sight distance analysis on three-dimensional highway alignments, *Transportation Research Record*, 1523(1): 1–10.
Iglesias-Martinez, L.; Castro, M., Pascual Gallego, V; De Santos-Berbel, C. 2016. Estimation of Sight Distance on Highways with Overhanging Elements. In *Proceedings of the International Conference on Traffic and Transport Engineering*, Belgrade, Serbia.
Ismail, K.; Sayed, T. 2007 New Algorithm for Calculating 3D Available Sight Distance, *Journal of Transportation Engineering*, 133(10): 572–581.
Jung, J.; Olsen, M. J.; Hurwitz, D. S.; Kashani, A. G.; Buker, K. 2018. 3D Virtual Intersection Sight Distance Analysis Using Lidar Data. *Transportation Research Part C: Emerging Technologies* 86: 563–579.
Khattak, A.; Hallmark, S.; Souleyrette, R. 2003. Application of Light Detection and Ranging Technology to Highway Safety, *Transportation Research Record: Journal of the Transportation Research Board* 1836: 7–15.
Khattak, A. J.; Shamayleh, H. 2005. Highway Safety Assessment through Geographic Information System-Based Data Visualization, *Journal of Computing in Civil Engineering*, 19(4): 407–411.
Ministerio de Fomento. 2016. *Norma 3.1-IC: Trazado*. Madrid: Ministerio de Fomento, Spain, 246 p.
Olsen, M. J.; Hurwitz, D.; Kashani, A.; Buker, K. 2016. 3D Virtual Sight Distance Analysis Using Lidar Data, Final Project Report. Pacific Northwest Transportation Consortium (PacTrans), Seattle, WA.
Trimble. 2018. SketchUp. Available from internet:<https://www.sketchup.com/es/products/sketchup-free>.